ISSN 1392–124X (print), ISSN 2335–884X (online) INFORMATION TECHNOLOGY AND CONTROL, 2015, T. 44, Nr. 3

A Collaborated Multi-controller Strategy by Using $\mathcal{L}_1$ Adaptive Augmentation Control for Power-generation Systems with Uncertainties

Lei Pan, Jiong Shen

Southeast University, School of Energy and Environment,
Key Laboratory of Energy Thermal Conversion and Control of Ministry of Education,
Si Pai Lou Str. 2, 210096 Nanjing, China
e-mail: panlei@seu.edu.cn, shenj@seu.edu.cn

Chengyu Cao

University of Connecticut, Department of Mechanical Engineering,
Auditorium Rd. 191, Storrs, CT 06269-3139, USA
e-mail: ccao@engr.uconn.edu

crossref http://dx.doi.org/10.5755/j01.itc.44.3.8846

Abstract. For dealing with uncertain operation circumstances, a collaborated multi-controller strategy of the cascade architecture with a $\mathcal{L}_1$ adaptive augmentation controller and a conventional baseline controller is introduced to power-generation systems. For its arbitrarily close, fast, and robust tracking performance, the $\mathcal{L}_1$ adaptive output feedback controller is designed as the augmentation controller in the inner-loop to keep the nominal dynamics of the system in the overall operation scope. The robust PID controller and offset-free linear MPC controller are recommended as the available outer-loop baseline controllers to follow control commands. The closed-loop stability of the cascade control system is ensured. The simulation experiments on a benchmark nonlinear boiler-turbine generation model verify the greatly improved adaptation and robustness of the augmentation control system in the presence of unknown uncertainties. Additionally, it is easy to upgrade a conventional control system to this cascade one in practice because the add-in $\mathcal{L}_1$ adaptive augmentation controller influences little on the augmented system setup.

Keywords: $\mathcal{L}_1$ adaptive controller; linear controller; uncertainty; nonlinearity; power plants.

1. Introduction

Nowadays, power-generation units inevitably operate in uncertain circumstances due to the disturbances caused by the intermittent emission control, the fluctuations of lower heating value (LHV) of fuel and the uncertain power supply by other renewable energy in grids. Their existing control systems usually cannot handle these uncertainty issues well and may lead to unstable operations. No doubt it is significant for power plants to improve the adaptation and robustness of their controllers for dealing with unknown uncertain conditions.

There are many control approaches in literatures on handling disturbances and modeling mismatch. A general state-space disturbance model is presented in [1] for the linear model predictive control (MPC). Based on the detectability conditions of the augmented disturbance model, steady-state offset caused by modeling error and unmeasured disturbances can be eliminated by the combined functions of the estimator, the steady-state target calculation, and the dynamic controller. Along this way, Maeder et al. [2] studied that the model only needs to be augmented by as many states as the tracked variables when tracking an asymptotically constant reference. Using the fuzzy models and an integrated disturbance model which accounts for all plant-model mismatch and un-modeled disturbances, Zhang et al. [3] developed an effective offset-free output feedback predictive control approach for nonlinear processes. Recent years, another kind of robust adaptive control approaches has attracted our sights. The $\mathcal{L}_1$ adaptive control is a class of robust adaptive control methods which offer guaranteed robustness with fast adaptation [4]. The fundamental theory of the $\mathcal{L}_1$ adaptive control is introduced in [5-8]. $\mathcal{L}_1$ adaptive control has been successfully applied to unmanned flight controls

having nonlinearities, time-varying disturbances, unknown parameters and un-modeled dynamics. Therefore, we have studied the $\mathcal{L}_1$ adaptive control strategy for the nonlinear boiler-turbine systems with internal un-modeled dynamics, time-varying parameters and unknown disturbances in our previous work [9], which shows that the proposed $\mathcal{L}_1$ adaptive controller guarantees good control quality for the power generation process in the presence of unknown uncertainties.

However, it may be unrealistic to fulfill the $\mathcal{L}_1$ adaptive controllers independently in large-scale power units. Because there are many coupled chemical loops in such sophisticated thermodynamic systems, it is difficult to replace all the conventional controllers by the novel advanced controllers. One feasible way is to augment the $\mathcal{L}_1$ adaptive controller into the conventional control systems for dealing with unknown uncertainties. This augmentation control strategy may be more reliable with less parameter modifications on the existing control systems to obtain a better control quality and thus has great practical significance. Therefore, we propose a collaborated multi-controller strategy for power-unit systems with severe nonlinearity, bounded disturbances and unknown uncertainties in this paper, i.e. the approach of the $\mathcal{L}_1$ adaptive augmentation controller collaborating with baseline controllers like PID or MPC. In this strategy, the $\mathcal{L}_1$ adaptive controller is augmented as an inner-loop controller in cascade with the baseline controller for compensating all the unknown disturbances and uncertainties. Among many kinds of $\mathcal{L}_1$ adaptive control methods, an extension approach of the $\mathcal{L}_1$ adaptive output feedback control [10] to systems of unknown relative degree is very suitable to make the augmentation controller. This approach adopts a new piece-wise continuous adaptive law along with the low-pass filtered control signal. It allows for achieving arbitrarily close tracking of the reference signals, and the transfer function of its reference system is not required to be strictly positive real. Stability of this system is guaranteed by its design via small-gain type argument. These features show that this $\mathcal{L}_1$ adaptive control approach may have great potential to be applied in wide industrial processes. Moreover, we will take two kinds of wide-applied baseline controllers for the augmented cascade-loop design and verifications, one is the robust PID controller; another is the offset-free linear MPC. We will make them to be augmented by the $\mathcal{L}_1$ adaptive output feedback controller and then to be used as the rapid coordinated tracking control system of the power-generation systems with severe nonlinearities, internal un-modeled dynamics, time-varying unknown disturbances and parameters.

In this collaborated multi-controller strategy, the $\mathcal{L}_1$ adaptive augmentation controller and the baseline linear controller collaborate together but are independent in the algorithms and even in hardware. Any existing controller in power units can be augmented by an inner-loop $\mathcal{L}_1$ adaptive controller to compensate the unknown uncertainties with little modifications on the existing controller parameters and then obtain enhanced control quality. It can be programmed in an independent controller from its partner linear controller, and only simple connections are made for them. Thus the $\mathcal{L}_1$ adaptive augmentation controller has great advantage for the real implementations.

The remainder of the paper is organized as follows. In Section 2, we propose the cascade control architecture and design the inner-loop $\mathcal{L}_1$ adaptive augmentation controller. In Section 3, a classic nonlinear boiler-turbine model is introduced for the study. In Section 4, two kinds of linear controllers with robust stability are introduced as the outer-loop baseline controllers. In Section 5, several simulation scenarios about wide-range load tracking with severe nonlinearity and unmatched model parameters are conducted to evaluate the performances of the collaborated multi-controller strategy of two kinds of baseline controllers and the $\mathcal{L}_1$ adaptive augmentation controller. In Section 6, we draw the conclusions for the study.

2. Cascade architecture of $\mathcal{L}_1$ adaptive augmentation controller and baseline controller

The baseline controllers like PID and MPC are widely applied in power units. It has real significance for power stations to enhance their baseline controllers by augmenting $\mathcal{L}_1$ adaptive output feedback controller to compensate nonlinearities, time-varying disturbances, model mismatch and un-modeled dynamics in the power generation process. The augmentation control architecture is shown in Fig. 1.

In this architecture, the baseline controller is designed for one working point, usually the nominal point. The $\mathcal{L}_1$ adaptive augmentation controllers are used to maintain the desired system performance defined by the nominal baseline controller close-loop dynamics, in the presence of nonlinearities, time-varying disturbances, model mismatch and un-modeled dynamics in the overall operation range. Under this objective, the $\mathcal{L}_1$ adaptive augmentation controller uses a fast adaptation algorithm to estimate the un-modeled uncertainties, and then it outputs a band-limited augmentation control signal by its control law to compensate the disturbances and model mismatch from the nominal working point. The total control signal is

$$u(t) = u_b(t) + u_c(t) \tag{1}$$

where $u_b(t)$ denotes the output of the baseline controller, and $u_c(t)$ denotes the output of the $\mathcal{L}_1$ adaptive augmentation controller. When the inner-loop dynamics tends to the nominal model for designing

the baseline controller, the augmentation control signal produced by the $\mathcal{L}_1$ adaptive control law tends to zero.

$\mathcal{L}_1$ adaptive augmentation controller and the baseline controller are independent of each other in algorithms. The design of the $\mathcal{L}_1$ adaptive augmentation controller is presented in this section.

2.1. Problem formulation

We describe the controlled plant dynamics as follows:

$$\begin{aligned} &\dot{x}(t) = A_m x(t) + B_m u(t) + f(x,z,t), x(0) = x_0, \\ &\dot{z}(t) = g(z,x,t), z(0) = z_0, \\ &y(t) = C_m^T x(t) \end{aligned} \tag{2}$$

where $x(t) \in R^n$ is the system state vector(measurable), $u(t) \in R^m$ is the input vector($m \le n$), $y(t) \in R^m$ is the output vector, $A_m \in R^{n\times n}$ is a known Hurwitz matrix, $B_m \in R^{n\times m}$ is a known full-rank constant matrix, $C_m \in R^{m\times n}$ is a known full-rank constant matrix, (A_m, B_m, C_m) defines the desired dynamics for closed-loop system, (A_m, B_m) is controllable, (A_m, C_m) is observable, zeros of $C_m^T(SI-A_m)^{-1}B_m$ lie in the open left-half s plane, $z(t) \in R^p$ is the immeasurable state vector of internal un-modeled dynamics, and $f: R^n \times R^p \times R \to R^n$ and $g: R^n \times R^p \times R \to R^p$ are unknown nonlinear functions.

The control objective is to design an augmentation adaptive output feedback controller, $u(t)$, such that the system output - $y(t)$ - tracks the desired system output $y_{des}(t)$ with desired transient and asymptotic performance. The desired system is described by

$$\begin{aligned} &\dot{x}_{des}(t) = A_m x_{des}(t) + B_m u_{des}(t), \\ &y_{des}(t) = C_m^T x_{des}(t) \end{aligned} \tag{3}$$

where (A_m, B_m, C_m) represents the nominal dynamics of the controlled plant in this approach.

2.2. $\mathcal{L}_1$ adaptive augmentation controller

$\mathcal{L}_1$ Adaptive controller consists of the state predictor, the adaptation law and the control law.

1) **State predictor.** The state predictor is given by:

$$\begin{aligned} &\dot{\hat{x}}(t) = A_m \hat{x}(t) + B_m u(t) + \hat{\sigma}(t) \\ &\hat{y}(t) = c_m^T \hat{x}(t), \hat{x}(0) = x_0 \end{aligned}, \tag{4}$$

where $\hat{x}(t) \in R^n$ and $\hat{y}(t) \in R^m$ are the state and output of the predictor respectively; $\hat{\sigma}(t) \in R^n$ compensates the system disturbances and model mismatch. We can find a constant matrix, $B_{um} \in R^{n\times(n-m)}$, such that $B_m^T B_{um} = 0$ and rank($[B_m \ \ B_{um}]$) = n. Then, equation (4) can be written as

$$\begin{aligned} &\dot{\hat{x}}(t) = A_m \hat{x}(t) + B_m(u(t) + \hat{\sigma}_1) + B_{um}\hat{\sigma}_2, \\ &\hat{y}(t) = c_m^T \hat{x}(t), \hat{y}(0) = y_0 \end{aligned} \tag{5}$$

where $\hat{\sigma}_1(t)$ represents the matched component of $\hat{\sigma}(t)$, and $\hat{\sigma}_2(t)$ represents the unmatched component.

2) **Adaptation law.** $\hat{\sigma}(t)$ is on-line estimated by the following adaptation law:

$$\begin{aligned} &\hat{\sigma}(t) = \hat{\sigma}(iT) \quad t \in [iT, (i+1)T], \\ &\hat{\sigma}(iT) = -\Phi^{-1}(T)\mu(iT), \quad i = 0,1,2,\ldots \end{aligned} \tag{6}$$

where $T>0$ is the integration time of the adaptation law; and

$$\begin{aligned} &\Phi(T) \triangleq \int_0^T e^{\Lambda A_m \Lambda^{-1}(T-\tau)} \Lambda d\tau, \\ &\mu(iT) = e^{\Lambda A_m \Lambda^{-1} T} 1_1 \tilde{y}(iT), \quad i = 0,1,2,\ldots \end{aligned} \tag{7}$$

where $\mathbf{1}_1 \in \mathrm{R}^N$ is the basis vector with first element **1** and all other elements zero; $\tilde{y}(t) \triangleq \hat{y}(t) - y(t)$; $\Lambda \triangleq \begin{bmatrix} c_m^T \\ D\sqrt{P} \end{bmatrix}, \Lambda \in R^{N\times N}$ where $P=P^T>0$ satisfies the algebraic Lyapunov equation

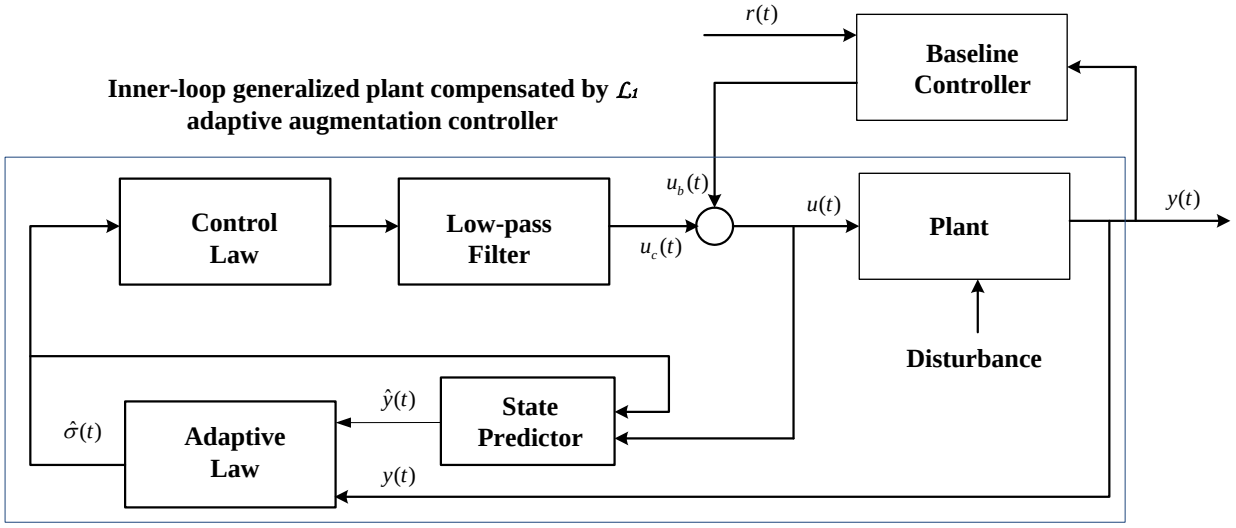

Figure 1. Cascade architecture of baseline controller and $\mathcal{L}_1$ adaptive augmentation controller

$A_m^T P + P A_m = -Q$, $Q > 0$; and $D \in R^{(N-1)\times N}$ satisfies $D(c_m^T(\sqrt{P})^{-1})^T = 0$.

3) **Control law.** The control law is defined as follows:

$$\begin{bmatrix} \hat{\sigma}_1(t) \\ \hat{\sigma}_2(t) \end{bmatrix} = [B_m \quad B_{um}]^{-1} \hat{\sigma}(t).$$

The augmentation control signal is given via the output of the low-pass filter $C(s)$:

$$u_c(s) = -C(s)(\hat{\sigma}_1(s) + M(s)\hat{\sigma}_2(s)), \tag{8}$$

where the $\mathcal{L}_1$ adaptive augmentation controller output $u_c(t)$ is the inverse Laplace transform of $u_c(s)$; $C(s)=KD(s)(I_m+KD(s))^{-1}$ is a strictly-proper stable low-pass filter matrix with DC gain $C(0) = I_m$, $K \in R^{m\times m}$ is a gain matrix, $D(s)$ is a $m \times m$ strictly-proper transfer function matrix (the choice of K and $D(s)$ needs to ensure that $C(s)M(s)$ is proper and stable), $\hat{\sigma}_1(s)$ and $\hat{\sigma}_2(s)$ are the Laplace transformations of $\hat{\sigma}_1(t)$ and $\hat{\sigma}_2(t)$, respectively. $M(s)$ is defined by

$$M(s) = (C_m^T(s)H_{xm}(s))^{-1}(C_m^T(s)H_{xum}(s)), \tag{9}$$

$$\begin{aligned} H_{xm}(s) &= (SI_n - A_m)^{-1}B_m, \\ H_{xum}(s) &= (SI_n - A_m)^{-1}B_{um}. \end{aligned} \tag{10}$$

The above piece-wise continuous adaptive law with the low-pass filtered control signal allows for achieving arbitrarily close tracking of the input and the output signals of the reference system. The performance bounds between the closed-loop reference system and the closed-loop $\mathcal{L}_1$ adaptive system can be rendered arbitrarily small by reducing the step size of integration. It can be represented by the following equations:

$$\lim_{T\to 0} y(t) = y_{ref}(t), \qquad \lim_{T\to 0} u(t) = u_{ref}(t). \tag{11}$$

The proof of the feasibility and stability of the above method can be found in [11].

Remark 1. With a fast-sampling $\mathcal{L}_1$ adaptive augmentation controller, all the disturbances and model-plant mismatch in the baseline controller loops can be estimated out and timely compensated, and thus the inner loop including $\mathcal{L}_1$ adaptive augmentation controller and the plant can perform a desired dynamics for the baseline controllers to control. The sampling time T should be small enough for $\mathcal{L}_1$ adaptive augmentation controller to achieve a timely compensation on the desired dynamics.

2.3. Closed-loop Stability

Assume that a precise compensation for the model mismatch is made by the $\mathcal{L}_1$ adaptive augmentation controller, namely the inner loop maintains the nominal dynamics in the presence of unknown uncertainties. Then the closed-loop stability and transient performance of the cascade system depends on the outer-loop baseline controller. It's not difficult to choose a stable linear controller, e.g. many PID controllers and stable MPC controllers.

Because the sampling frequency of the $\mathcal{L}_1$ adaptive augmentation controller is much higher than that of the baseline controller, the stability of the inner loop is ensured by the $\mathcal{L}_1$ - gain stability condition [7] of the $\mathcal{L}_1$ adaptive augmentation controller which can be satisfied by designing a proper filter. The tracking performance bounds between the desired dynamics and the inner-loop dynamics can be rendered arbitrarily small by reducing the integration step size of the $\mathcal{L}_1$ adaptive augmentation controller, the proof can be found in [8,11]. Therefore, one should make the sampling time T of the inner loop small enough so that the tracking bounds can be tolerated by the baseline controller in the sense of its stability margin.

In a word, the stability of the cascade system can be guaranteed by a $\mathcal{L}_1$ adaptive augmentation controller which satisfies the $\mathcal{L}_1$ - gain stability condition and its fast-sampling which makes the tracking bounds of the inner loop to the nominal dynamics small enough within the stability margin of a nominal stable baseline controller.

3. Dynamic model of a nonlinear boiler-turbine-generator unit

Before we design the $\mathcal{L}_1$ adaptive augmentation control system for power-generation units, we introduce the nonlinear boiler-turbine-generator unit model of Bell and Åström [12] to be the controlled plant in our study in this section. This model was derived specifically for a steam boiler with a turbine in a power plant unit. Due to its capability of capturing the key characteristics of real boiler-turbine systems, including multiple variables, nonlinearity, unmeasured internal state, strong coupling, large inertia, non-minimum phase, and unstable plant etc., this model has been widely used in literature as a benchmark for control studies [13-18], and has also been chosen by us for developing and verifying the $\mathcal{L}_1$ adaptive augmentation control approach. A schematic picture of the boiler–turbine system is shown in Fig. 2. The steam boiler part converts the input chemical energy of fuel into the thermal energy that is directly fed to the turbine part and is converted into the mechanical energy and then the electricity energy in the generator finally.

The model is a third-order multiple input multiple output nonlinear dynamic equation group, described as follows:

$$\begin{cases} \dot{x}_1 = -0.0018u_2 x_1^{9/8} + 0.9u_1 - 0.15u_3 \\ \dot{x}_2 = (0.073u_2 - 0.016)x_1^{9/8} - 0.1x_2 \\ \dot{x}_3 = [141u_3 - (1.1u_2 - 0.19)x_1]/85 \\ y_1 = x_1 \\ y_2 = x_2 \\ y_3 = 0.05(0.1307x_3 + 100a_{cs} + q_e/9 - 67.975) \end{cases} \tag{12}$$

where the state variables are drum steam pressure x_1 in units of kg/cm^2, electric power x_2 in MW and drum/riser fluid density x_3 in kg/cm^3. The output variables y_1 and y_2 are the same as x_1 and x_2; the output y_3 in units of *meter* denotes the drum water level deviation, where evaporation rate α_{cs} in kg and steam quality q_e in kg/s are given by

$$q_e = (0.854u_2 - 0.147)x_1 + 45.59u_1 - 2.514u_3 - 2.096, \quad (13)$$

$$a_{cs} = \frac{(1-0.001538x_3)(0.8x_1 - 25.6)}{x_3(1.0394 - 0.0012304x_1)}. \quad (14)$$

The input variables include the normalized fuel flow rate u_1 (0-1 corresponds to 0-14kg/s), control valve position of steam to the turbine u_2 (0-1) and normalized feedwater flow rate u_3 (0-1 corresponds to 0-14kg/s). The inputs are subject to magnitude and rate saturations as follows:

$$0 \le u_i \le 1, i = 1,2,3$$

$$-0.007 \le \dot{u}_1 \le 0.007$$

$$-2 \le \dot{u}_2 \le 0.002$$

$$-0.005 \le \dot{u}_3 \le 0.05. \quad (15)$$

Its verified working points are shown in Table 1. The nominal one is marked as #2.

4. $\mathcal{L}_1$ adaptive augmentation control system for nonlinear boiler-turbine-generator units

Based on the cascade architecture of augmentation control shown in Fig. 1, we will design the $\mathcal{L}_1$ adaptive augmentation control system for the nonlinear boiler-turbine-generator unit. We take two typical kinds of controllers often used in the power plants to be the baseline controllers in the augmentation control system. One is the robust PID; another is the offset-free linear MPC (OFL-MPC). They are representative for the conventional control and the advanced control approaches, respectively.

Table 1. Equilibrium operating points of the boiler-turbine dynamics

	#1	#2	#3	#4
$\mathbf{x_1}$	75.6	108	129.6	135.4
$\mathbf{x_2}$	15.27	66.65	105.8	127
$\mathbf{x_3}$	299.6	428	513.6	556.4
$\mathbf{u_1}$	0.156	0.34	0.505	0.6
$\mathbf{u_2}$	0.483	0.69	0.828	0.8971
$\mathbf{u_3}$	0.183	0.433	0.663	0.793
$\mathbf{y_3}$	-0. 97	0	0.64	0.98

4.1. $\mathcal{L}_1$ adaptive augmentation control system I: $\mathcal{L}_1$ adaptive controller and robust PID controller

A robust PID controller in [13] has shown its good performance in the wide-range load-tracking process of the nonlinear boiler-turbine-generator model (12)-(15) and thus been well-known. It is designed from the loop-shaping H_∞approach by using a linearized model at the nominal operating point. A precompensator and postcompensator were designed with a constant decoupler, aligning the singular values of the model at 0.001 *rad/s*. The resulting H_∞ controller is then transformed into four SISO PI controllers by using a

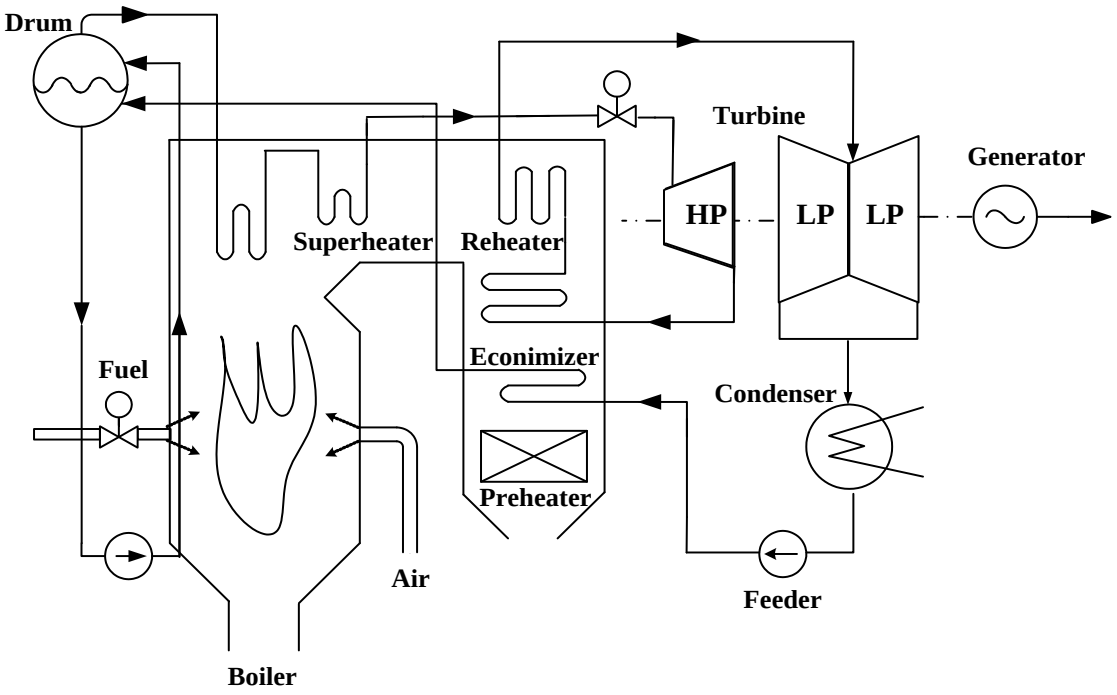

Figure 2. Schematic of a boiler-turbine-generator unit

PID reduction method. The anti-windup bumpless transfer (AWBT) technique is employed after the PID controller design to compensate for the effect of the constraints. The final form of the AWBT PI controllers will be easy for its real application. Here the PI controller has the form $k(s) = k(1+1/\tau_I S)$ and the four PI controllers are given by

$$K(s)=\begin{bmatrix} 0.0485+\frac{0.0012}{s} & 0 & 1.2091+\frac{0.0486}{s} \\ 0 & 0.0197+\frac{0.0045}{s} & 0 \\ 0 & 0 & 7.2548+\frac{0.2914}{s} \end{bmatrix}. \quad (16)$$

The schematic of an anti-windup PI controller is shown in Fig. 3 [12].

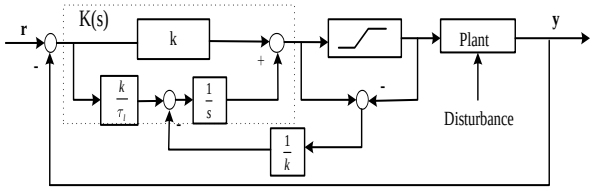

Figure 3. One AWBP PI controller

The AWBP PI controllers have very limited tolerance in parameter perturbations and disturbances. We enhance it with the $\mathcal{L}_1$ adaptive augmentation controller as shown in Fig. 4.

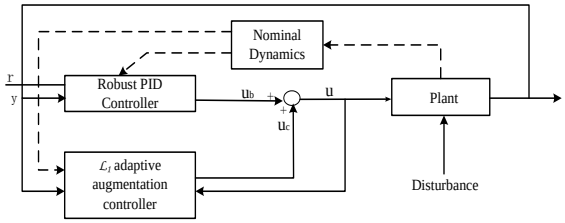

Figure 4. Robust PID and $\mathcal{L}_1$ adaptive augmentation control scheme

4.2. $\mathcal{L}_1$ adaptive augmentation control system II: $\mathcal{L}_1$ adaptive controller and OFL-MPC

For achieving energy-saving and safe operation in the power-generation process, many PID controllers in power plants have been upgraded into MPC controllers due to their successfully solving the control problems with long delay, with coupled inputs and with constraint optimization. The OFL-MPC [1,2] is an efficient control approach in constrained linear processes for its performances on output tracking without steady-state offset, stability guarantee and disturbance rejections. But it cannot deal with the severe nonlinear dynamics and large model-plant mismatch. We introduce this approach in the following and then test its performance under unknown uncertain conditions without and with a $\mathcal{L}_1$ adaptive augmentation controller, respectively, in the simulations.

The OFL-MPC is composed of three components: an augmented observer with estimated disturbance signals, an online constrained target generator and an input-to-state stabilizing predictive controller. Its nominal plant model is the same as the desired model of the $\mathcal{L}_1$ adaptive augmentation controller, i.e.

$$\begin{aligned} \dot{x}(t) &= A_m x(t) + B_m u(t), \\ y(t) &= c_m^T x(t) \end{aligned} \quad (17)$$

which is discretized into

$$\begin{cases} x(k+1) = Ax(k) + Bu(k) \\ y(k) = Cx(k) \end{cases}. \quad (18)$$

The OFL-MPC approach lumps the mismatch and disturbances into the augmented states to make a disturbance model as follows

$$\begin{aligned} \begin{bmatrix} x(k+1) \\ d(k+1) \end{bmatrix} &= \begin{bmatrix} A & E \\ 0 & 1 \end{bmatrix} \begin{bmatrix} x(k) \\ d(k) \end{bmatrix} + \begin{bmatrix} B \\ 0 \end{bmatrix} u(k) \\ y(k) &= \begin{bmatrix} C & F \end{bmatrix} \begin{bmatrix} x(k) \\ d(k) \end{bmatrix}. \end{aligned} \quad (19)$$

The observability of the disturbance model (19) is given in Lemma 1[2].

Lemma 1. *The disturbance model presented in (18) is detectable if and only if (C, A) is detectable and*

$$rank \begin{bmatrix} (I-A) & -E \\ C & F \end{bmatrix} = n + n_d, \quad (20)$$

where n is the number of the nonaugmented states, n_d is the number of the disturbances.

1. **Augmented Observer**. Consider the following observer

$$\begin{aligned} \begin{bmatrix} \hat{x}(k+1) \\ \hat{d}(k+1) \end{bmatrix} &= \begin{bmatrix} A & E \\ 0 & I \end{bmatrix} \begin{bmatrix} \hat{x}(k) \\ \hat{d}(k) \end{bmatrix} + \begin{bmatrix} B \\ 0 \end{bmatrix} u(k) + \begin{bmatrix} L_1 \\ L_2 \end{bmatrix} [\hat{y}(k) - y(k)] \\ \hat{y}(k) &= \begin{bmatrix} C & F \end{bmatrix} \begin{bmatrix} \hat{x}(k) \\ \hat{d}(k) \end{bmatrix} \end{aligned} \quad (21)$$

where the observer gain $L = [L_1^T \quad L_2^T]^T$ is determined by the pole placement.

2. **Target generator**. In order to remove the effects from the disturbances estimation $\hat{d}(k)$, the state and input targets x_t and u_t are computed by solving the following quadratic program (QP):

$$\begin{aligned} &\min_{x_t, u_t} [(y_t - y_s)^T Q_t (y_t - y_s) + (u_t - u_s)^T R_t (u_t - u_s)] \\ &s.t. \\ &\begin{bmatrix} I-A & -B \\ C & 0 \end{bmatrix} \begin{bmatrix} x_t \\ u_t \end{bmatrix} = \begin{bmatrix} E\hat{d}(k) \\ -F\hat{d}(k) + y_s \end{bmatrix} \\ &u_{\min} \le u_t \le u_{\max} \\ &y_{\min} \le Cx_t + F\hat{d}(k) \le y_{\max} \end{aligned} \quad (22)$$

where y_s is the desired output reference, u_s is the steady-state manipulated variable profile, (u_{min},u_{max}) and (y_{min},y_{max})are the input and output constraints, respectively.

3. **Prediction model**. With the feasible solutions of (22), the multi-step-ahead state and output prediction models are given by

$$\bar{Z}(k) = T_A Z(k) + T_B W(k), \tag{23}$$

$$\bar{Z}(k+N \mid k) = A_N Z(k) + A_B W(k), \tag{24}$$

where $Z(k)=x(k)-x_t$. Let $Z(k|k)=Z(k)$, and

$$\bar{Z}(k) = \begin{bmatrix} Z(k \mid k) \\ z(k+1 \mid k) \\ \cdot \\ \cdot \\ \cdot \\ Z(k+N-1 \mid k) \end{bmatrix}; \text{ Let } \omega=u-u_t, \text{ and}$$

$$W(k) = \begin{bmatrix} \omega(k \mid k) \\ \omega(k+1 \mid k) \\ \cdot \\ \cdot \\ \cdot \\ \omega(k+N-1 \mid k) \end{bmatrix};$$

$$T_A = \begin{bmatrix} I_N \\ A_0 \\ \vdots \\ A_{N-1} \end{bmatrix}, T_B = \begin{bmatrix} 0 & \cdots & 0 & 0 \\ B_0 & \cdots & 0 & 0 \\ \vdots & \ddots & 0 & 0 \\ \prod_{j=0}^{N-3} A_{N-1-j} B_0 & \cdots & B_{N-2} & 0 \end{bmatrix}$$

$$A_N = \prod_{j=0}^{N-1} A_{N-1-j}, A_B = \left[\prod_{j=0}^{N-2} A_{N-1-j} B_0 \times \prod_{j=0}^{N-3} A_{N-1-j} B_1 \cdots A_{N-1} B_{N-2} B_{N-1} \right] \tag{25}$$

where N denotes the predictive horizon, $A_0=A$, $B_0=B$.

4. **Dynamic optimization problem**

For the disturbance model of Eq.(19) subject to the input constraints $u_{\min} \le u_t \le u_{\max}$ and detectable, the closed-loop output feedback predictive control system, with stable augmented observer (21) and feasible solutions of the target generator (22), is input-to-state stable and achieves the offset-free reference tracking performance if there exist feasible optimal solutions of a control sequence $W(k)$, a set of positive definite matrices $X(k)$ and $Y(k)$ to the dynamic optimization problem

$$\min_{r_1, r_2, W, \{X_s\}, \{Y_s\}} \left(r_1 + \rho r_2 \right) \tag{26}$$

subject to the linear matrix inequalities

$$\begin{bmatrix} r_1 & * & * \\ T_A \bar{x}(k) + T_B W & \tilde{Q}^{-1}/2 & * \\ W & 0 & \tilde{R}^{-1} \end{bmatrix} \ge 0,$$

$$\begin{bmatrix} 1/\rho & * \\ A_N \bar{x}(k) + A_B W & X \end{bmatrix} > 0,$$

$$\begin{bmatrix} (\theta/\rho) I_N & * \\ A_N & X \end{bmatrix} \ge 0,$$

$$\begin{bmatrix} X & * & * & * \\ AX + BY & X & * & * \\ X & 0 & \rho r_2 Q^{-1} & * \\ Y & 0 & 0 & \rho r_2 R^{-1} \end{bmatrix} > 0,$$

$$\begin{bmatrix} \bar{u}_j^2 & U_j Y \\ Y^T U_j^T & X \end{bmatrix} \ge 0, \; j = 1, \ldots, m,$$

$$\begin{bmatrix} I_{m \times n} \\ -I_{m \times n} \end{bmatrix} W(k) \le \begin{bmatrix} \Pi_m (u_{\max} - u_t) \\ -\Pi_m (u_{\min} - u_t) \end{bmatrix},$$

where $\bar{x}(k) = \hat{x}(k) - x_t, \tilde{Q} = I_N \otimes Q, \tilde{R} = I_N \otimes R, \theta$ is a given design parameter, $\rho = \left(1 + \sqrt{\theta} e_x\right), e_x$ is the upper bound on the state estimation error, $\Pi_m = \left[I_m \ldots I_m \right]^T$,

$\bar{u}_j = \min \left\{ \left| u_{\max} - u_t \right|_j, \left| u_{\min} - u_t \right|_j \right\}$,

$U_j = [0 \quad \ldots \quad 0 \quad 1 \quad 0 \quad \ldots \quad 0], \; j = 1, \ldots, m$.

Based on the linear predictive model and the disturbance observer, the above OFL-MPC controller can tolerate small model-plant mismatch, but it isn't adaptive to large un-modeled dynamics. We enhance it by a $\mathcal{L}_1$ adaptive augmentation controller as shown in Fig. 5.

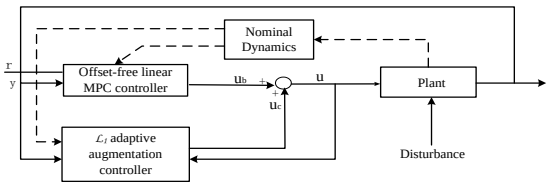

Figure 5. OFL-MPC and $\mathcal{L}_1$ adaptive augmentation control scheme

5. Simulations and Discussion

In order to verify the cascade control algorithm, we will make several simulation experiments on the boiler-turbine model of Eq. (12)-(15). We design the $\mathcal{L}_1$ adaptive augmentation controller based on (4), (6), (7) and (8) for the nonlinear boiler-turbine model. The design information is shown as follows.

Linearizing the nonlinear B-A model (1) at the #2 equilibrium point, we get the state-space model coefficients as follows for designing the state predictor of the $\mathcal{L}_1$ adaptive augmentation controller:

$$A_m = \begin{bmatrix} -0.0025 & 0 & 0 \\ 0.0694 & -0.1 & 0 \\ -0.0067 & 0 & 0 \end{bmatrix},$$

$$B_m = \begin{bmatrix} 0.9 & -0.349 & -0.15 \\ 0 & 14.155 & 0 \\ 0 & -1.398 & 1.659 \end{bmatrix},$$

$$C_m = \begin{bmatrix} 1 & 0 & 0 \\ 0 & 1 & 0 \\ 0.0063 & 0 & 0.0047 \end{bmatrix},$$
$$D_m = \begin{bmatrix} 0 & 0 & 0 \\ 0 & 0 & 0 \\ 0.2533 & 0.5124 & -0.014 \end{bmatrix}. \quad (27)$$

Let the inner-loop sampling time T=0.01s equal to one percent of the outer-loop linear controller sampling time T_s=1, which makes the inner-loop $\mathcal{L}_1$ adaptive augmentation controller compensate the model-process mismatch timely and precisely. We make two baseline controllers collaborate with the $\mathcal{L}_1$ adaptive augmentation control. One is a robust PID controller; another is the OFL-MPC controller. The resulting cascade systems are presented in Section 4 and shown in Fig. 4 and 5. We take the filter as $C(s)$ = $0.1/(s+0.1)$ in the robust PID augmentation controller and $C(s)$ = $25/(s^2+14s+25)$ in the OFL-MPC augmentation controller, respectively.

For a clear performance comparison between the linear control systems with and without the $\mathcal{L}_1$ adaptive augmentation controller, we make a large variation of the coefficients and the power in the nonlinear dynamic model of Eq. (12). The changed model is shown in Eq. (28):

$$\frac{dP}{dt} = 0.9u_1 - 0.0036u_2P^{9/8} - 0.15u_3$$
$$\frac{dE}{dt} = ((0.73u_2 - 0.16)P^{12/8} - E)/10 \quad (28)$$
$$\frac{d\rho_f}{dt} = (282u_3 - (2.2u_2 - 0.19)P)/85.$$

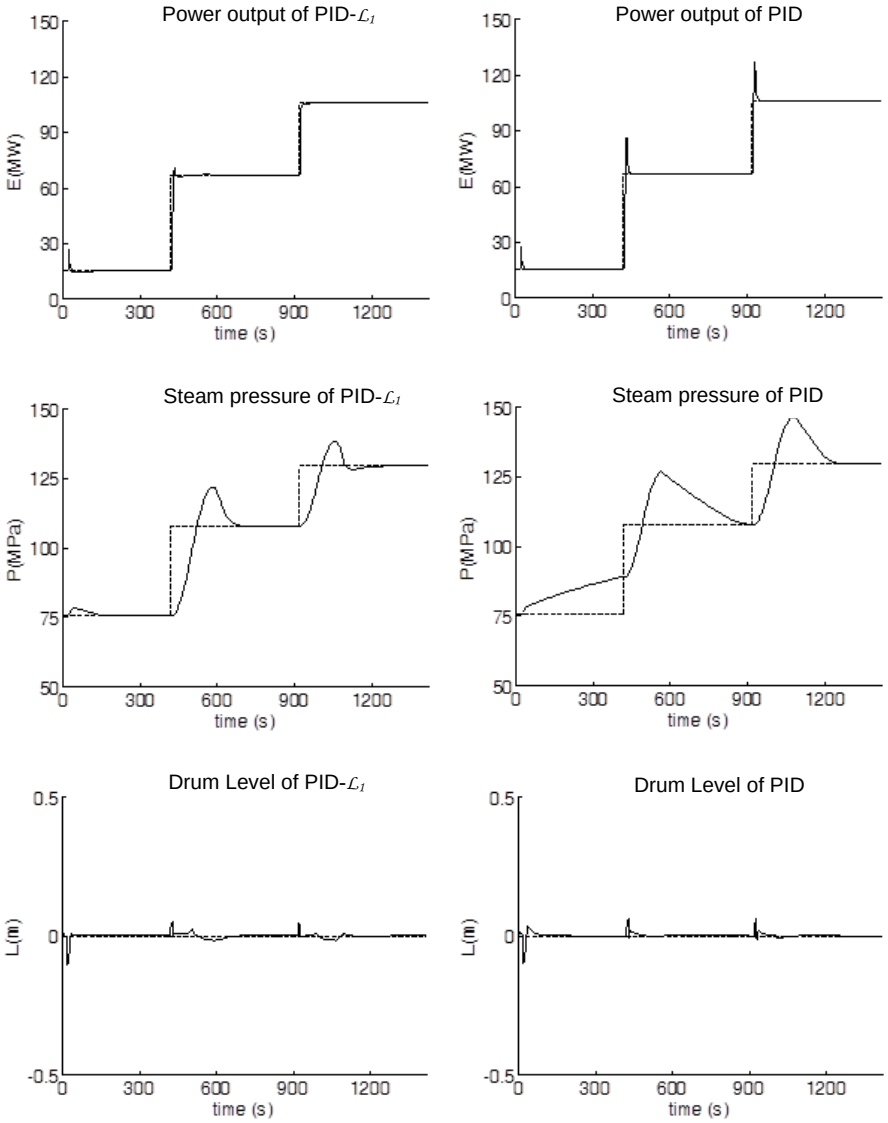

Figure 6. Comparison on the output variables from PID-L1 augmentation loops (left) and single PID loop (right) (solid line: output; dotted line: set-point)

5.1. PID-$\mathcal{L}_1$ adaptive augmentation control system

We make two wide-range load tracking operations and show the results in Fig. 6 for output variables and Fig. 7 for manipulated variables. For comparing each pair of the same variables in parallel, the output variables from the cascade robust PID-$\mathcal{L}_1$ augmentation adaptive control loops are shown on the left side in Fig. 6, and the output variables from the single robust PID controller loop are shown on the right side in Fig. 6. When the simulation time instant t=20s, let the boiler-turbine model change from the previous one into Eq. (28). The tracking results are shown in Fig. 6 and 7. From the output results in Fig. 6, we can see that the performance of the robust PID alone degrades greatly when large parameter variation of the plant arises. The PID-$\mathcal{L}_1$ augmentation controller shows good adaptivity to such unknown uncertainty as seen in the left-side sub figures in Fig. 6, due to the timely compensation by the signal u_c from the output of the $\mathcal{L}_1$ augmentation controller presented by the dash-dot curve shown in the left-side sub figures of Fig. 7. The signal u_c of the robust PID-alone loop keeps zero as seen in the right-side sub figures of Fig. 7 because the $\mathcal{L}_1$ augmentation controller is disconnected from the system. Therefore, the cascade PID-$\mathcal{L}_1$ augmentation controller works much better than the robust PID controller alone for the processes with unknown uncertainties. The $\mathcal{L}_1$ adaptive augmentation controller is very effective.

5.2. MPC-$\mathcal{L}_1$ adaptive augmentation control system

We design the OFL-MPC controller based on (21)-(26). The observer gain L is obtained by the pole placement for the augmented system (20). The placed poles are [-0.09, -0.09, -0.12, 0.12, -0.135, -0.165]^T. Other design parameters are chosen as Q_t =

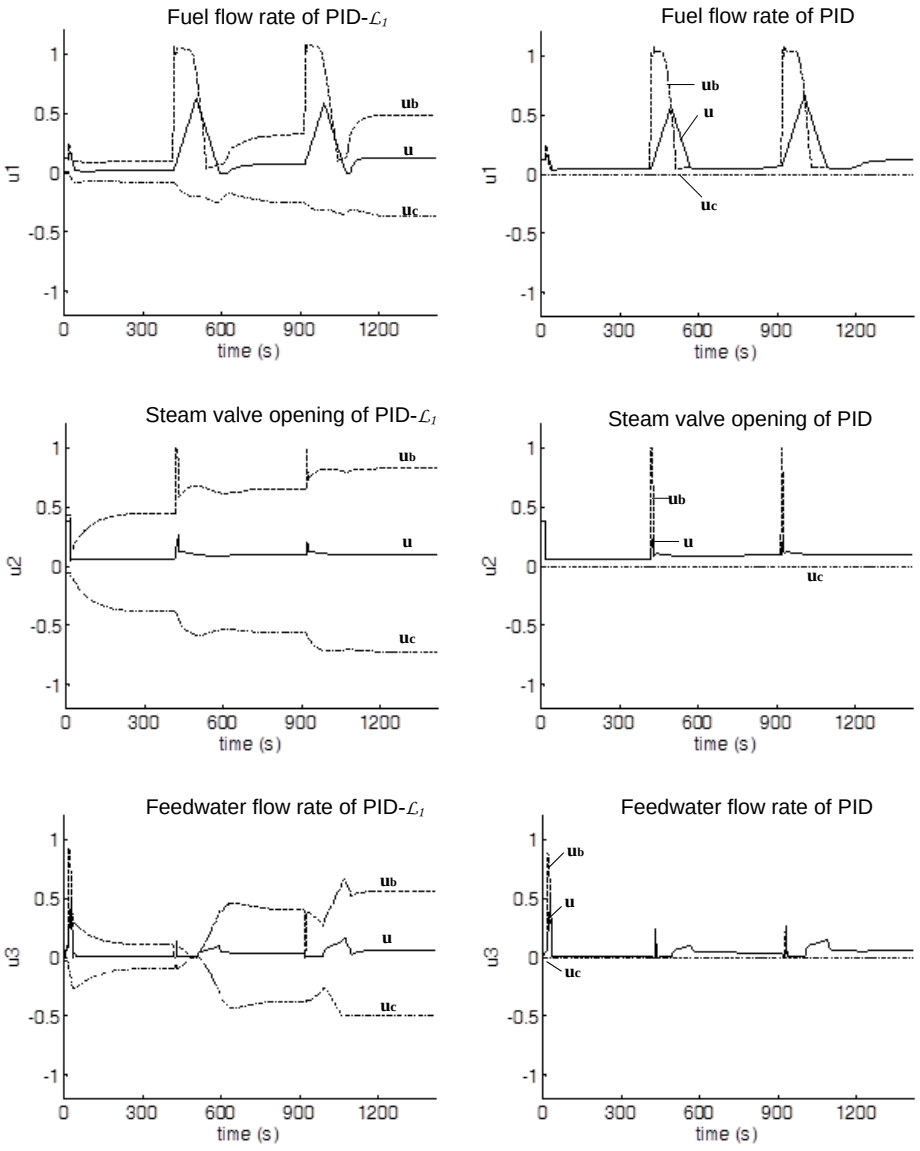

Figure 7. Comparison on the manipulated variables from PID-L1 augmentation controller (left) and PID controller (right); Each total control signal u = ub +uc s.t. Eq.(15)

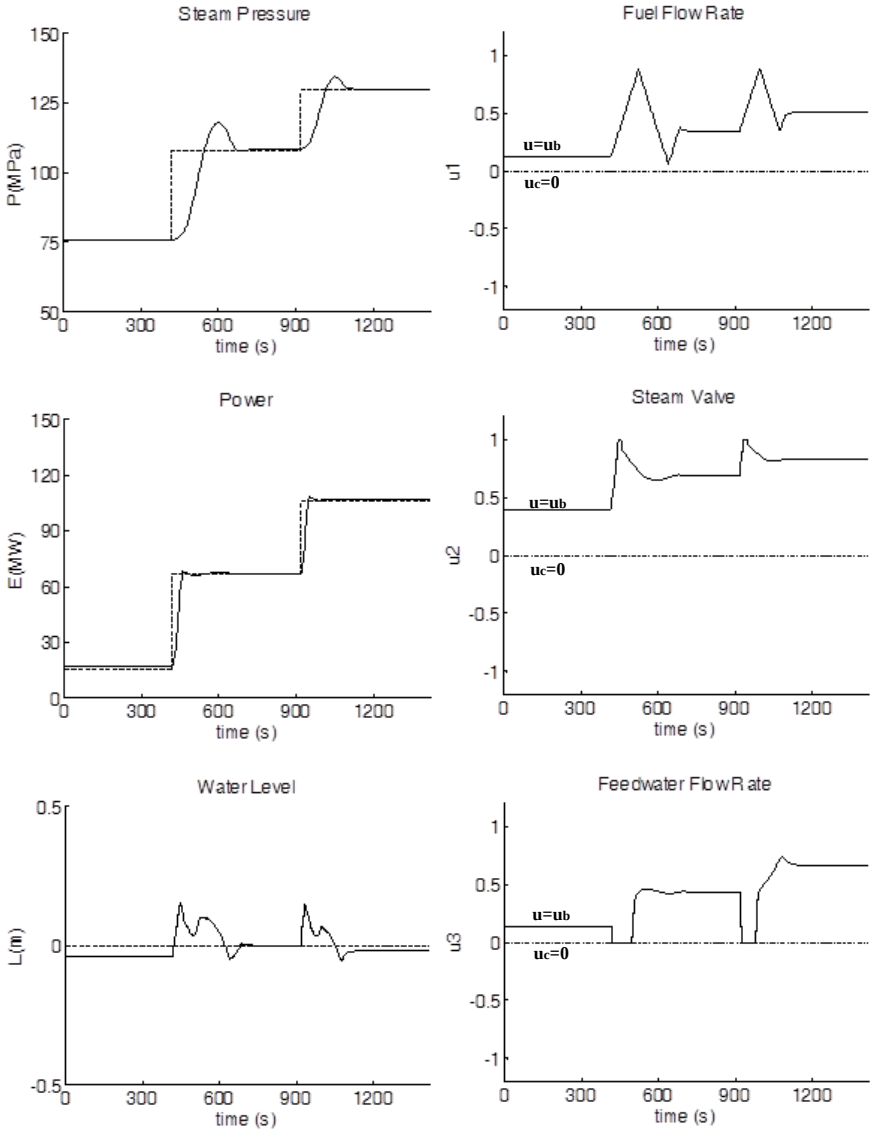

Figure 8. The results of the signle MPC loop without uncertainties
Left: output variables (solid line: output; dotted line: set-point); Right: manipulated variables

$R_t = I_3$, $Q = 0.5 \cdot I_3$, $R = 150 \cdot I_3$, θ=40, e_x=10, the predictive horizon N=10, which is affordable on optimization computing time. Two simulation scenarios are made for the evaluation.

Case 1: The wide-range load tracking only by the MPC controller without uncertainty in the process. The results are shown in Fig. 8. This OFL-MPC we design has good robustness on the nonlinearity in a wide load range.

Case 2: The wide-range load tracking with varying of the model parameters as shown in Eq. (28) at the time instant t=120s. Fig. 9 shows the comparison on the output variables from the single MPC loop and the OFL-MPC-$\mathcal{L}_1$ augmentation loops. The sub figures on the left side in Fig. 9 show the output variables from the single Offset-free linear MPC loop. When the MPC controller works alone, it cannot deal with severe nonlinearity and unknown uncertainty. The system looks critical stable at both the medium and high load points. Whereas, the sub figures on the right side in Fig. 9 show stable and good control performance of the OFL-MPC-$\mathcal{L}_1$ augmentation loops all the range. When the MPC controller and the $\mathcal{L}_1$ adaptive augmentation controller collaborate in the cascade loop, the obvious compensating control signals of the fuel flow rate, the steam valve and the feed-water flow rate are produced by the $\mathcal{L}_1$ adaptive augmentation controller, as shown in the right-side sub figures of Fig. 10. Each total control signal $u = u_b + u_c$ *s.t.* (15) of u_1, u_2, u_3 makes the closed-loop system stable all the range. Fig. 10 shows the comparison on the manipulated variables from the single OFL-MPC loop and the OFL-MPC-$\mathcal{L}_1$ augmentation loops.

Comparing the two cases, we know that the OFL-MPC cannot keep the system stable in wide-range operation with the parameter variations of the plant. But with the augmentation of the $\mathcal{L}_1$ adaptive output feedback controller, it can control the nonlinear process with unknown uncertainties very well.

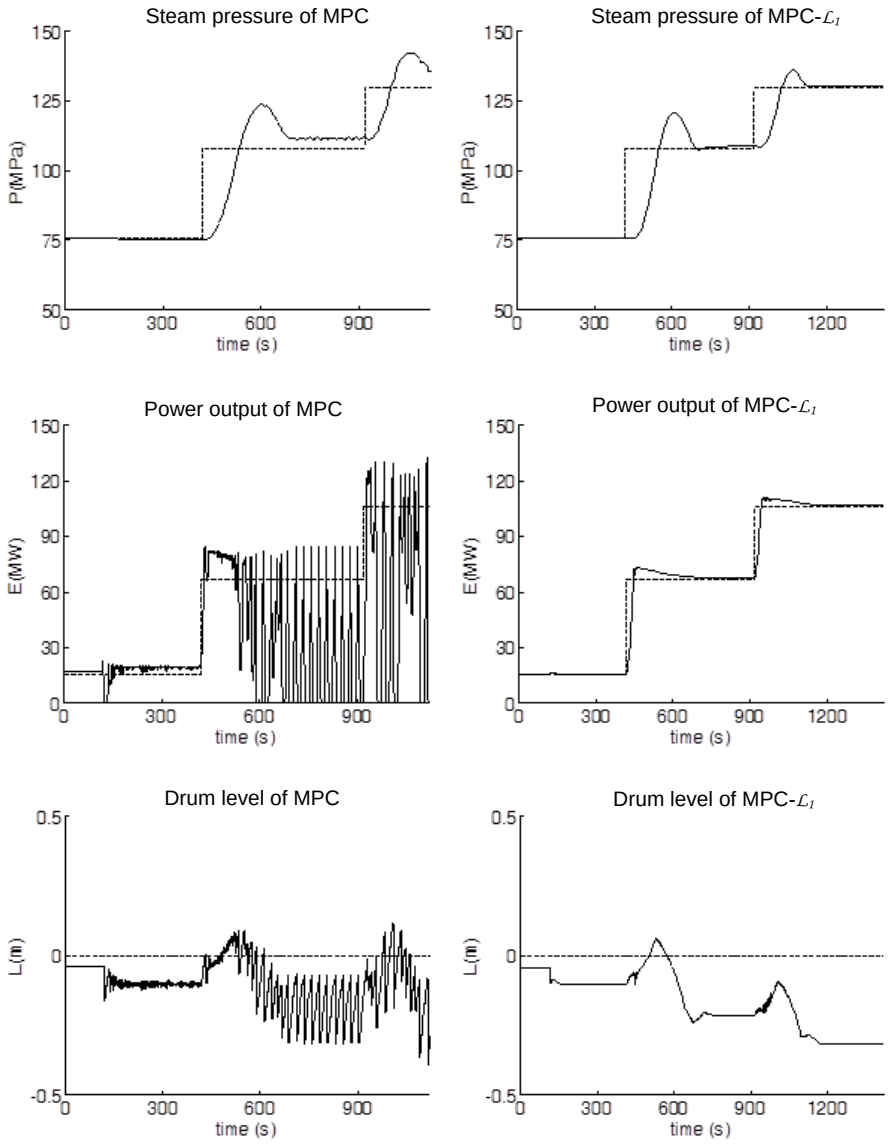

Figure 9. Comparison on the output variables of single OFL-MPC loop (left) and OFL-MPC-$\mathcal{L}_1$ augmentation loops (right) in the presence of parameter variations (solid line: output; dotted line: set-point)

Remark 2. Both the robust PID controller and the OFL-MPC can work well in the nonlinear wide-range load tracking without uncertainties. Although the robust PID with AWBT function has better robustness than the OFL-MPC controller in terms of the unknown uncertainties in the simulations, both of their control qualities get much worse in this case. The simulations demonstrate that the $\mathcal{L}_1$ adaptive augmentation controller can effectively handle uncertainties including unmatched model, unmeasured disturbances and severe nonlinearity. This collaboration of the linear controllers and the $\mathcal{L}_1$ adaptive augmentation controller has much better adaptation and robustness than the baseline controller alone for nonlinear systems.

We don't change any parameter of the baseline controllers when the $\mathcal{L}_1$ adaptive augmentation controller is connected into the loops in the simulations above. The low-pass filter of the $\mathcal{L}_1$ adaptive augmentation controller, which needs to ensure the $\mathcal{L}_1$ -gain condition [7], should be designed individually for different loops. Thus we have two different filters in the cascade PID-$\mathcal{L}_1$ adaptive augmentation controller and the MPC-$\mathcal{L}_1$ adaptive augmentation controller.

6. Conclusions

Most of the existing controllers for power generation units cannot maintain good performances as some uncertainties arise in the process. This paper proposes an augmentation control scheme to improve the adaptation and robustness of the linear controllers serving in power generation processes. For its arbitrarily close tracking performance and fast, robust adaptation, the $\mathcal{L}_1$ adaptive output feedback control

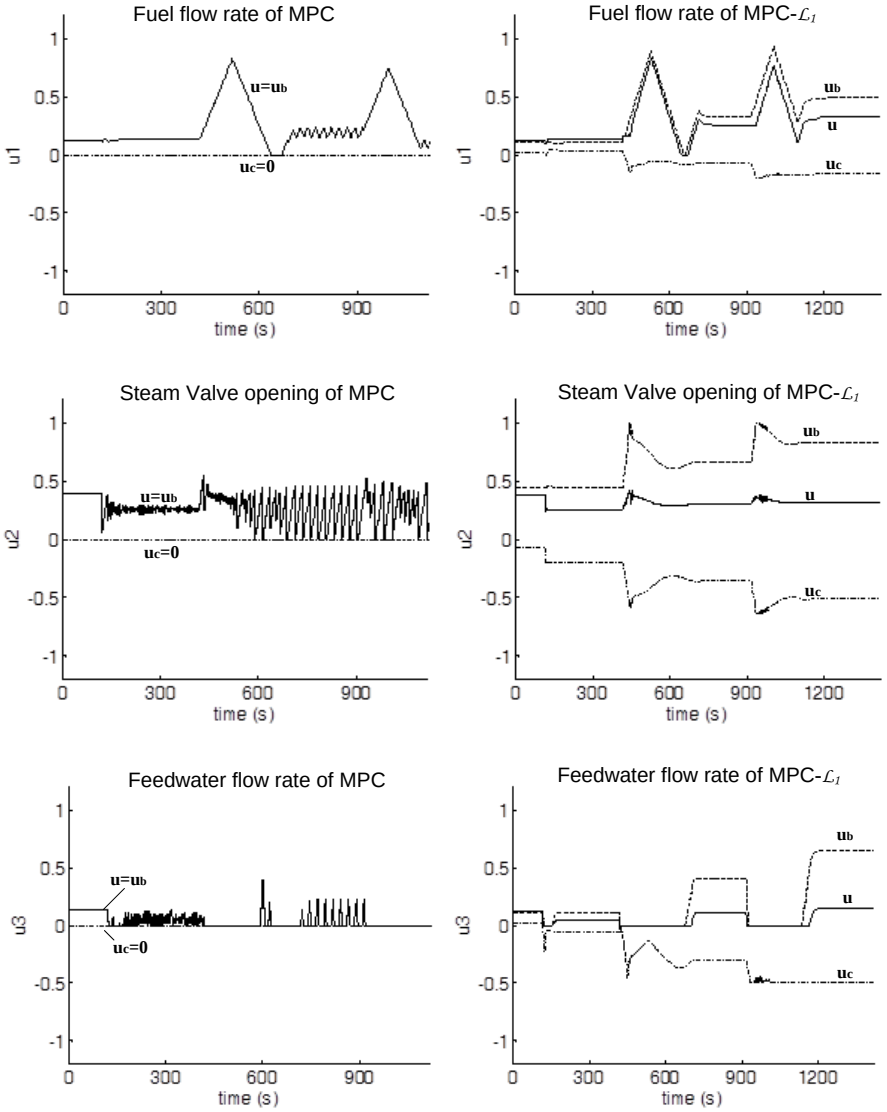

Figure10. Comparison on the manipulated variables of single MPC loop (left) and OFL-MPC-$\mathcal{L}_1$ augmentation loops (right) in the presence of parameter variations

approach is designed into the augmentation controller which takes effect and help with the linear controllers in the presence of uncertain conditions in the power-generation process. In this augmentation control scheme, the baseline controller, the $\mathcal{L}_1$ adaptive augmentation controller and the plant form a cascade control loop. A $\mathcal{L}_1$ adaptive output feedback controller and the plant form into the inner-loop equivalent to a general plant with the desired dynamics for the outer baseline controllers to control. This fast-sampling $\mathcal{L}_1$ adaptive augmentation controller estimates the uncertainties and makes up their influence on the controlled process quickly. Because the transient tracking performance bound of the $\mathcal{L}_1$ adaptive controller can be rendered arbitrary small by reducing the step size of integration, the stability of the cascade control system can be ensured by tuning the sampling time of the inner $\mathcal{L}_1$ adaptive controller loop small enough. Two common controllers used in power-generation process, the robust PID controller and offset-free linear MPC controller, are introduced and connected with the $\mathcal{L}_1$ adaptive augmentation controller in cascade. The simulation experiments on the boiler-turbine model with severe nonlinearity and time-varying parameters verify that the collaboration of the linear controllers and the $\mathcal{L}_1$ adaptive augmentation controller can greatly improve the closed-loop system stability under unknown uncertainties. Furthermore, it doesn't need to change any parameter of the baseline controllers when a $\mathcal{L}_1$ adaptive output feedback controller is connected into the augmentation control system. It gives the great advantage for the real implementation because it doesn't take much time and cost to upgrade the controller for handling unknown uncertainties. Therefore we conclude that the coordinated multi-controller strategy by using the $\mathcal{L}_1$ adaptive augmentation controller can be accepted as a novel

promotion scheme for the control performance under unknown uncertainties in power plants.

Acknowledgments

This work was supported by the National Natural Science Foundation of China under Grant 51106024. The authors would like to express their appreciations to all the editors and reviewers for their precious time and work on this paper.

References

[1] **K. R. Muske, T. A. Badgwell.** Disturbance modeling for offset-free linear model predictive control. *Journal of Process Control*, 2002, Vol. 12, No. 5, 617-632.

[2] **U. Maeder, F. Borrelli, M. Morari.** Linear offset-free model predictive control. *Automatica*, 2009, Vol. 45, No. 10, 2214-2222.

[3] **T. J. Zhang, G. Feng, X. J. Zeng.** Output tracking of constrained nonlinear processes with offset-free input-to-state stable fuzzy predictive control. *Automatica*, 2009, Vol. 45, No. 4, 900-909.

[4] **C. Cao, N. Hovakimyan.** Design and analysis of a novel $\mathcal{L}_1$ adaptive control architecture with guaranteed transient performance. *IEEE Transactions on Automatic Control*, 2008, Vol. 53, No. 4, 586-591.

[5] **C. Cao, N. Hovakimyan.** $\mathcal{L}_1$ adaptive controller for a class of systems with unknown nonlinearities: part I. In: *Proceedings of the American control conference, ACC*, Seattle, WA, United states, 2008, pp. 4093-4098.

[6] **C. Cao, N. Hovakimyan.** $\mathcal{L}_1$ adaptive controller for nonlinear systems in the presence of unmodelled dynamics: Part II. In: *Proceedings of the American control conference, ACC, Seattle, WA, United states*, 2008, pp. 4099-4104.

[7] **C. Cao, N. Hovakimyan.** Stability margins of $\mathcal{L}_1$ adaptive control architecture. *IEEE Transactions on Automatic Control*, 2010, Vol. 55, No. 2, 480-487.

[8] **N. Hovakimyan, C. Cao.** $\mathcal{L}_1$ adaptive control theory: guaranteed robustness with fast adaptation. *SIAM*, 2010.

[9] **J. Luo, L. Pan, C. Cao.** L_1 adaptive controller for a nonlinear boiler-turbine system. In: *Proceedings of the 53rd Annual ISA POWID Symposium, Summerlin, NV, United states*, 2010.

[10] **C. Cao, N.Hovakimyan.** $\mathcal{L}_1$ adaptive output-feedback controller for non-strictly-positive-real reference systems: missile longitudinal autopilot design. *Journal of Guidance, Control, and Dynamics*, 2009, Vol. 32, 717-726.

[11] **C. Cao, N. Hovakimyan.** $\mathcal{L}_1$ adaptive output feedback controller for systems of unknown dimension. *IEEE Transactions on Automatic Control*, 2008, Vol. 53, No. 3, 815-821.

[12] **R. Bell, K. J. Åström.** Dynamic models for boiler–turbine alternator units: data logs and parameter estimation for a 160MW unit. *Technical Report, Department of Automatic Control, Lund Institute of Technology, Sweden*, 1987.

[13] **W. Tan, H. J. Marquez, T. Chen, J. Liu.** Analysis and control of a nonlinear boiler-turbine unit. *Journal of Process Control*, 2005, Vol. 15, No. 8, 883-891.

[14] **P. Chen, J. Shamma.** Gain-scheduled $\mathcal{H}_2$-optimal control for boiler–turbine dynamics with actuator saturation. *Journal of Process Control*, 2004, Vol. 14, 263-277.

[15] **U. C. Moon, K. Y. Lee.** Step-response model development for dynamic matrix control of a drumtype boiler–turbine system. *IEEE Transactions on Energy Conversion*, 2009, Vol. 24, No. 2, 423-430.

[16] **J. Wu, J. Shen, M. Krug, S. K. Nguang, Y. G. Li.** GA-based nonlinear predictive switching control for a boiler-turbine system. *Journal of Control Theory and Applications*, 2012, Vol. 10, 100-106.

[17] **M. Keshavarz, M. B. Yazdi, M. R. Jahed-Motlagh.** Piecewise affine modeling and control of a boiler-turbine unit. *Applied Thermal Engineering*, 2010, Vol. 30, No. 8, 781-791.

[18] **Y. G. Li, J. Shen, K. Y. Lee, X. C. Liu.** Offset-free fuzzy model predictive control of a boiler-turbine system based on genetic algorithm. *Simulation Modelling Practice and Theory*, 2012, Vol. 26, 77-95.

Received December, 2014.